Title
Ongoing oroclinal bending in the Cascadia forearc and its relation to concave-outboard plate margin geometry

Journal
Geology, 47(2)

ISSN
0091-7613

Authors
Finley, Theron
Morell, Kristin
Leonard, Lucinda
et al.

Publication Date
2019-02-01

DOI
10.1130/g45473.1

Peer reviewed

Publisher: GSA
Journal: GEOL: Geology
DOI:10.1130/G45473.1

Ongoing oroclinal bending in the Cascadia forearc and its relation to concave-outboard plate margin geometry

Theron Finley[1,2], Kristin Morell[1,3], Lucinda Leonard[1], Christine Regalla[4], Stephen T. Johnston[2], and Wenbo Zhang[1,2]

[1]*School of Earth and Ocean Sciences, University of Victoria, 3800 Finnerty Road, Victoria, BC V8P 5C2, Canada*

[2]*Department of Earth and Atmospheric Sciences, University of Alberta, 1-26 Earth Sciences Bldg., Edmonton, AB T6G 2E3, Canada*

[3]*Department of Earth Sciences, University of California, Santa Barbara, 1006 Webb Hall, Santa Barbara, California, 93106, USA*

[4]*Department of Earth and Environment, Boston University, 685 Commonwealth Avenue, Boston, Massachusetts 02215, USA*

ABSTRACT

The concave-inboard geometry of most convergent margins is considered a natural consequence of the depression of the edge of a thin spherical cap, whereas concave-outboard margin segments often form around indenters on the subducting plate. At the Cascadia subduction zone, the apex of a >500-km-long concave-outboard bend in the trench presently shows no obvious subduction of an indenter but does coincide with the axis of an outboard-facing concavity in upper plate rocks arched around the Olympic Peninsula in northwestern Washington, USA. Here we synthesize paleomagnetic and structural data together with new analyses of GNSS data to show that the upper plate at Cascadia has been folded from Miocene to

Recent into an orocline with an axial trace that bisects the Olympic Peninsula. The processes that accommodate bending, which we suggest include folding by flexural slip on the orocline limbs, and shortening, uplift and escape within the core of the fold at the Olympic Mountains, have the combined result of relative motion of the forearc towards the arc at the core of the orocline, and sustained opposing rotations of the upper plate on the orocline limbs. We propose that oroclinal bending is promoted and maintained by along-strike variations in plate boundary tractions resulting from the geometry of the plate interface at depth and suggest that these processes can contribute to the development of concave-outboard margins without the need for a subducting indenter.

INTRODUCTION

The geometry and shape of convergent margins and consequent variations in relative plate motion influence a number of important seismogenic processes, including the distribution of locking on the plate interface (e.g., Wang et al., 2003) and strain partitioning between the megathrust and the overriding plate (e.g., Yu et al., 1993). The broad concave-inboard geometry of most convergent margins is considered a natural consequence of the depression of the edge of a thin spherical cap (e.g., Mahadevan et al., 2010), while syntaxial concave-outboard margin segments often form around a subducting indenter such as an oceanic plateau or seamount chain (e.g. Bendick and Ehlers, 2014; Marshak, 2004). Along the eastern margin of the Pacific Ocean, there are several >500-km-long concave-outboard convergent margin sections (Bolivia, Panama, and Cascadia, Fig. 1) that presently show no obvious subduction of an indenter, but do show evidence for past or present oroclinal bending within the upper plate near the apex of the trench concavity (e.g. Silver et al., 1990; Allmendinger et al., 2005a; Johnston and Acton, 2003). In the case of the "Bolivian orocline" (Fig. 1, BOL), GNSS (Global Navigational Satellite System) and paleomagnetic data together demonstrate that oroclinal bending has been occurring continuously since at least 26 Ma (Allmendinger et al., 2005a). These observations suggest that oroclinal bending may be an important process in the long-term evolution of concave-outboard convergent margins over long spatial wavelengths.

Here we focus on a region of the Cascadia subduction zone where, similar to the Bolivian case, the apex of a >500-km-long concave-outboard bend in the trench (Fig. 2A) appears coincident with the axis of an outboard-facing concavity in upper plate rocks arched around the Olympic Peninsula (Fig. 2B) (Beck and Engebretson, 1982; Brandon and Calderwood, 1990; Warnock et al., 1993). We use paleomagnetic and structural data to show that oroclinal bending is responsible for their arcuate shape, and use geodetic data to show that the upper plate has been folding from at least Miocene to Recent into an orocline. We propose that ongoing oroclinal bending has led to the development of the concave-outboard geometry of Cascadia due to along-strike variations in plate boundary tractions imposed by the geometry of the lower plate.

EVIDENCE FOR PAST AND PRESENT OROCLINAL BENDING AT CASCADIA

Paleomagnetic and Structural Constraints on Post-Eocene Bending

Inboard of the trench concavity at Cascadia (Fig. 2A), ophiolitic basalts of the Crescent-Siletz terrane form an arcuate belt around the eastern periphery of the Olympic Mountains (Fig. 2B). This arcuate pattern has long been recognized, but its origin is debated (Cady, 1975; Brandon and Calderwood, 1990; Warnock et al., 1993) and the timing of its formation has previously been restricted to the Eocene (Johnston and Acton, 2003). Oroclinal bending, where an originally linear belt is bent around a vertical axis to form a curved map pattern (Carey, 1955), predicts opposing senses of vertical axis rotation on each orocline limb, and parallelism between foliations and paleomagnetic declinations within the orocline (Eldredge et al., 1985).

Observations in the Cascadia forearc provide evidence for both of these predictions. First, paleomagnetic declinations measured in rocks of the Eocene Crescent-Siletz terrane and the overlying Oligocene Sooke Formation (Beck and Engebretson, 1982; Warnock et al., 1993; Prothero et al., 2008) record clockwise rotation to the south of the Olympic Peninsula, compared to counterclockwise rotation to the north (Fig. 2B). These data indicate an average of 22º of post-Eocene rotation, with a reversal of rotation sense located near the axial trace of the geologically-defined orocline in the Crescent-Siletz terrane (Fig. 2B). Second, structural data collected from both the Crescent-Siletz terrane and the Olympic core complex (Washington Geological Survey, 2017) reveal a systematic along-strike change shared among paleomagnetic declinations and the strike of regional foliations (Fig. 2B, Fig. DR1 in the GSA Data Repository[1]). These relationships suggest that the arcuate shape of the Crescent-Siletz terrane has resulted from post-Eocene bending of an originally linear belt, as predicted by an orocline model (e.g. Eldredge et al., 1985).

Geodetic Constraints on Contemporary Bending

To test whether oroclinal bending is occurring in the Cascadia forearc today, we calculated vertical axis rotations using processed GNSS velocity data from 282 continuous and 641 campaign sites, with average time series lengths of 10.3 years and 6.5 years, respectively (Figure 2A; UNAVCO Plate Boundary Observatory (https://www.unavco.org/data/gps-gnss/gps-gnss.html), and McCaffrey et al., 2013). We first used an adaptive Gaussian smoothing function (Mazzotti et al., 2011) to interpolate crustal velocity across a 0.2º x 0.2º grid. Annual rotation rates were then derived by calculating the curl of the smoothed velocity field at each grid point (see Data Repository for details).

The analysis of GNSS velocity data shows ~0.5-2 °/Myr of contemporary rotation on each limb of the Olympic orocline, with a distinct northward transition from clockwise to counterclockwise across the Olympic Peninsula (Fig. 3 and Table DR1). The switch in rotation sense correlates spatially with both the reversal in rotations recorded by paleomagnetic declinations and with the geologically-defined axial trace of the orocline (Fig. 2B). These spatial similarities suggest that, rather than being solely related to Eocene processes (e.g. Johnston and Acton, 2003), oroclinal bending has been continuous through time, recorded in the long term (>10 Myr) by geologic and paleomagnetic data (Fig. 2B), and in the short term (>10 years) by the GNSS vertical axis rotations (Fig. 3). Moreover, although the GNSS velocity field of the Cascadia forearc is strongly influenced by interseismic strain due to megathrust locking (e.g., Wang et al., 2003), the correlation between short-term and long-term vertical axis rotations in the forearc implies that a portion of upper plate crustal strain occurring during the megathrust interseismic period results in permanent crustal deformation.

OROCLINAL BENDING PROCESSES AT CASCADIA

Based on our synthesis of paleoseismic, geodetic, geomorphic, and thermochronologic data, we suggest that oroclinal bending at Cascadia is accommodated via a combination of flexural slip (Donath and Parker, 1964), orthogonal flexure (Bobillo-Ares et al., 2000), and fold-axis parallel extrusion (Dietrich, 1989), wherein transpression with opposite slip sense occurs on the orocline limbs and compression occurs within the orocline core (Fig. 2B). Paleoseismic data show that Quaternary fault kinematics are dominantly right-lateral-transpressional to the north of the orocline, and left-lateral-transpressional to the south (e.g., Nelson et al., 2017). At the core of the orocline, the Olympic Mountains exhibit upper plate shortening (Mazzotti et al., 2002), lateral material escape (Nelson et al. 2017), and high rates of uplift and incision (Pazzaglia and Brandon, 2001)—processes that are expected within the core of an actively developing fold.

We suggest that the geometry of the subducting slab, and resulting spatial variations in plate boundary tractions, are key factors in promoting and maintaining oroclinal bending at Cascadia. In map view, the axial trace of the orocline is subparallel to the hinge of a broad arch (upward convexity) in the subducting slab (Fig. 4). The gentler subduction angle at this slab arch hinge leads to a locally lower thermal gradient along the plate interface, and a consequently wider locked zone beneath the Olympic Peninsula (Fig. 2A) (e.g., Wang et al., 2003). This configuration results in GNSS crustal velocities that are greatest near the orocline core (~20 mm/yr), and decrease to the north and south to ~10 mm/yr (Fig. 2A). These north-south gradients in forearc motion promote oroclinal bending by imparting opposing shear strain on opposite limbs of the orocline.

Given the approximate spatial coincidence of the axial trace of the orocline with the slab arch hinge, we further suggest that oroclinal bending at Cascadia results from decoupling between margin-normal strain accommodated on the megathrust and slab-strike-parallel strain taken up within the forearc. The margin-parallel component of relative plate motion is right-lateral in sense south of the Olympic Peninsula and decreases to near-zero north of the peninsula, without a change in the sense of obliquity (Fig. 4). However, the component of relative plate motion parallel to slab strike at ~30-50 km depth on the plate interface changes sense across the slab arch hinge, near the axial trace of the orocline (Fig 4). Maximum horizontal compressive stress directions (S_{Hmax}) within the upper plate crust, calculated from crustal earthquake focal mechanisms and borehole breakouts (Balfour et al., 2011; Heidbach et al., 2016), trend subparallel to slab strike and fan around the Olympic Peninsula in a concave-outboard shape

(Fig. 4). Quaternary-active faults surrounding the core of the orocline have slip senses consistent with the kinematics predicted by this crustal stress field (Fig. 4 inset). These observations support the idea that forearc strain is dominated by slab-strike-parallel stresses that promote opposing senses of shear and rotation on the orocline limbs.

LONG-LIVED (>10 MYR) OROCLINAL BENDING AND ITS RELATIONSHIP TO MARGIN CONCAVITY

The alignment (within ~20 km distance and ~10-20° trend) of the geologically- (Fig. 2B) and geodetically-defined (Fig. 3) axial traces of the orocline suggests the processes that accommodate oroclinal bending, including flexural slip on the limbs, and shortening, uplift and escape within the orocline core, have persisted at the same position within the upper plate over a relatively long (>10 Myr) period of time. Assuming the Olympic orocline has persisted since at least the Miocene onset of uplift of the Olympic Mountains at ~18 Ma (Brandon et al., 1998), the paleomagnetic rotations measured in Eocene rocks imply an average rotation rate of |1.25| ± 1.0 °/Myr, which is comparable to the geodetically-derived contemporary average rotation rate of |0.96| ± 0.85 °/Myr (Fig. 3, Table DR1). If oroclinal bending at Cascadia is intrinsically related to both slab geometry and subduction obliquity, as we suggest, these results imply that the current along-strike variations in slab geometry and subduction obliquity have remained in the same position relative to the upper plate since at least the Miocene.

Although the initiation of bending may have been influenced by past margin geometry or the subduction of an indenter, we suggest that the concave-outboard geometry at Cascadia can be sustained by these persistent along-strike variations in slab geometry and subduction obliquity alone. The crustal processes associated with oroclinal bending should result in relative arcward motion of the trench along the axial trace of the orocline, and relative seaward rotation of the trench in the orocline limbs. Assuming that rates of influx of accreted sediment and outflux of eroded sediment at the trench are in equilibrium at all points along strike (Pazzaglia and Brandon, 2001), the long-lived opposing shear strain inherent to the geometry and kinematics of the plate margin will maintain a trench concavity that aligns with the axial trace of the orocline, as observed in Cascadia.

Similar patterns of vertical axis rotations, crustal shortening, relative plate motions and slab geometry occur at the apex of the ~5000-km-long concave-outboard bend in the South American margin near Bolivia. Much like Cascadia, long-lived and ongoing bending of the Bolivian orocline is recorded by paleomagnetic and GNSS vertical axis rotations, both of which are opposite in sign and similar in rate on each orocline limb (Allmendinger et al., 2005a). The axial trace of the Bolivian orocline also corresponds with both a convex-upward slab arch in the subducting Nazca plate (Hayes et al., 2012) and a reversal in subduction obliquity at the apex of the margin concavity. Kinematics of Plio-Quaternary faulting (Allmendinger et al., 2005b), and modelling of GNSS data (Bevis et al., 2001), suggest that margin-parallel shortening occurs on margin-normal faults in the core of the Bolivian orocline, in a similar manner to Cascadia. These similarities indicate that persistent oroclinal bending, related to slab geometry and subduction obliquity, may be a common characteristic of the upper plate at concave-outboard convergent margins.

CONCLUSIONS

We demonstrate, for the first time, that active bending of the Olympic orocline has persisted from at least Miocene (~18 Ma) to the present, and is accommodated by flexural slip on the orocline limbs, and crustal shortening, exhumation, and lateral escape within the orocline core. We observe a subparallelism in map view between the axial trace of the orocline and the hinge line of an arch in the subducting slab, indicating that oroclinal bending is maintained by opposing senses of shear on the orocline limbs due to variations in plate boundary tractions intrinsic to the geometry of the slab arch. Our results imply that the Cascadia margin, much like Bolivia, is an example of a long-lived orocline that has led to the development of a long-wavelength concave-outboard margin concavity, without the need for the subduction of an indenter in the present.

ACKNOWLEDGMENTS

Stephane Mazzotti provided a Fortran code for computing rotations from GNSS velocity data. Figures were created with the Generic Mapping Tools software (Wessel et al., 2013). We thank Yvette Kuiper, Jack Loveless, Dennis Brown, and an anonymous reviewer for comments that helped improve this manuscript. This research was partially supported by a University of Victoria Jamie Cassels Undergraduate Research Award to T.F., and by NSF grants EAR-1756834 and EAR-1756943.

REFERENCES CITED

Allmendinger, R.W., Smalley, R., Bevis, M., Caprio, H., and Brooks, B., 2005a, Bending the Bolivian orocline in real time: Geology, v. 33, p. 905–908, https://doi.org/10.1130/G21779.1.

Allmendinger, R.W., González, G., Yu, J., Hoke, G., and Isacks, B., 2005b, Trench-parallel shortening in the Northern Chilean Forearc: Tectonic and climatic implications: Bulletin of the Geological Society of America, v. 117, p. 89–104, doi:10.1130/B25505.1.

Balfour, N.J., Cassidy, J.F., Dosso, S.E., and Mazzotti, S., 2011, Mapping crustal stress and strain in southwest British Columbia: Journal of Geophysical Research, v. 116, p. B03314, https://doi.org/10.1029/2010JB008003.

Beck, M.E., and Engebretson, D.C., 1982, Paleomagnetism of small basalt exposures in the West Puget Sound Area, Washington, and Speculations on the accretionary origin of the Olympic Mountains: Journal of Geophysical Research, v. 87, p. 3755–3760, https://doi.org/10.1029/JB087iB05p03755.

Bendick, R., and Ehlers, T.A., 2014, Extreme localized exhumation at syntaxes initiated by subduction zone geometry: Geophysical Research Letters, v. 41, p. 5861–5867, https://doi.org/10.1002/2014GL061026.

Bevis, M., Kendrick, E., Smalley, R., Brooks, B., Allmendinger, R., and Isacks, B., 2001, On the strength of interplate coupling and the rate of back arc convergence in the central Andes: An analysis of the interseismic velocity field: Geochemistry, Geophysics, Geosystems, v. 2, doi:10.1029/2001GC000198.

Bobillo-Ares, N.C., Bastida, F., and Aller, J., 2000, On tangential longitudinal strain folding: Tectonophysics, v. 319, p. 53–68, https://doi.org/10.1016/S0040-1951(00)00026-3.

Brandon, M.T., and Calderwood, A.R., 1990, High-pressure metamorphism and uplift of the Olympic subduction complex: Geology, v. 18, p. 1252–1255, https://doi.org/10.1130/0091-7613(1990)018<1252:HPMAUO>2.3.CO;2.

Brandon, M.T., Roden-Tice, M.K., and Garver, J.I., 1998, Late Cenozoic exhumation of the Cascadia accretionary wedge in the Olympic Mountains, northwest Washington State: Geological Society of America Bulletin, v. 110, p. 985–1009, https://doi.org/10.1130/0016-7606(1998)110<0985:LCEOTC>2.3.CO;2.

Cady, W.M., 1975, Tectonic Setting of the Tertiary Volcanic Rocks of the Olympic Peninsula, Washington: Journal of Research of the U.S. Geological Survey, v. 3, p. 573–582.

Carey, S.W., 1955, The orocline concept in geotectonics: Part I: Papers and Proceedings of the Royal Society of Tasmania, v. 89, p. 255-288.

DeMets, C., Gordon, R.G., and Argus, D.F., 2010, Geologically current plate motions: Geophysical Journal International, v. 181, p. 1–80, https://doi.org/10.1111/j.1365-246X.2009.04491.x.

Dietrich, D., 1989, Fold-axis parallel extension in an arcuate fold- and thrust belt: The case of the Helvetic nappes: Tectonophysics, v. 170, p. 183–212, https://doi.org/10.1016/0040-1951(89)90271-0.

Donath, F.A., and Parker, R.B., 1964, Folds and Faulting: Geological Society of America Bulletin, v. 75, p. 45–62, https://doi.org/10.1130/0016-7606(1964)75[45:FAF]2.0.CO;2.

Eldredge, S., Bachtadse, V., and Van Der Voo, R., 1985, Paleomagnetism and the orocline hypothesis: Tectonophysics, v. 119, p. 153–179, https://doi.org/10.1016/0040-1951(85)90037-X.

Hayes, G.P., Wald, D.J., and Johnson, R.L., 2012, Slab1.0: A three-dimensional model of global subduction zone geometries: Journal of Geophysical Research. Solid Earth, v. 117, p. B01302, https://doi.org/10.1029/2011JB008524.

Heidbach, O., Rajabi, M., Reiter, K., and Ziegler, M., 2016, World Stress Map: World Stress Map Database Release, v. 2016, https://doi.org/10.5880/WSM.2016.001.0.

Johnston, S.T., and Acton, S., 2003, The Eocene Southern Vancouver Island Orocline — a response to seamount accretion and the cause of fold-and-thrust belt and extensional basin formation: Tectonophysics, v. 365, p. 165–183, https://doi.org/10.1016/S0040-1951(03)00021-0.

Li, G., Liu, Y., Regalla, C., and Morell, K.D., 2018, Seismicity relocation and fault structure near the Leech River fault zone, southern Vancouver Island: Journal of Geophysical Research. Solid Earth, v. 123, p. 2841–2855, https://doi.org/10.1002/2017JB015021.

Mahadevan, L., Bendick, R., and Liang, H., 2010, Why subduction zones are curved: Tectonics, v. 29, TC6002, https://doi.org/10.1029/2010TC002720.

Marshak, S., 2004, Salients, Recesses, Arcs, Oroclines, and Syntaxes — A Review of Ideas Concerning the Formation of Map-view Curves in Fold-thrust Belts: Thrust tectonics and hydrocarbon systems: American Association of Petroleum Geologists Memoir 82, v. 82, p. 131–156.

Mazzotti, S., Dragert, H., Hyndman, R.D., Miller, M.M., and Henton, J.A., 2002, GPS deformation in a region of high crustal seismicity: N. Cascadia forearc: Earth and Planetary Science Letters, v. 198, p. 41–48, https://doi.org/10.1016/S0012-821X(02)00520-4.

Mazzotti, S., Leonard, L.J., Cassidy, J.F., Rogers, G.C., and Halchuk, S., 2011, Seismic hazard in western Canada from GPS strain rates vs. earthquake catalog: Journal of Geophysical Research, v. 116, B08406, doi:https://doi.org/10.1029/2011JB008213.

McCaffrey, R., King, R.W., Payne, S.J., and Lancaster, M., 2013, Active tectonics of northwestern U.S. inferred from GPS-derived surface velocities: Journal of Geophysical Research. Solid Earth, v. 118, p. 709–723, https://doi.org/10.1029/2012JB009473.

McCrory, P.A., Blair, J.L., Waldhauser, F., and Oppenheimer, D.H., 2012, Juan de Fuca slab geometry and its relation to Wadati-Benioff zone seismicity: Journal of Geophysical Research, v. 117, p. B09306, https://doi.org/10.1029/2012JB009407.

Morell, K.D., Regalla, C., Leonard, L.J., Amos, C., and Levson, V., 2017, Quaternary rupture of a crustal fault beneath Victoria, British Columbia, Canada: GSA Today, v. 27, p. 4–10, https://doi.org/10.1130/GSATG291A.1.

Nelson, A.R., Personius, S.F., Wells, R.E., Bradley, L.A., Buck, J., Schermer, E.R., and Reitman, N., 2017, Holocene earthquakes of magnitude 7 during westward escape of the Olympic Mountains, Washington: Bulletin of the Seismological Society of America, v. 107, p. 2394–2415, https://doi.org/10.1785/0120160323.

Pazzaglia, F.J., and Brandon, M.T., 2001, A fluvial record of long-term steady-state uplift and erosion across the Cascadia forearc high, western Washington State: American Journal of Science, v. 301, p. 385–431, https://doi.org/10.2475/ajs.301.4-5.385.

Prothero, D.R., Draus, E., Cockburn, T.C., and Nesbitt, E.A., 2008, Paleomagnetism and counterclockwise tectonic rotation of the Upper Oligocene Sooke Formation, southern Vancouver Island, British Columbia: Canadian Journal of Earth Sciences, v. 45, p. 499–507, https://doi.org/10.1139/E08-012.

Silver, E.A., Reed, D.L., Tagudin, J.E., and Heil, D.J., 1990, Implications of the north and south Panama thrust belts for the origin of the Panama orocline: Tectonics, v. 9, p. 261–281, https://doi.org/10.1029/TC009i002p00261.

Wang, K., Wells, R., Mazzotti, S., and Hyndman, R.D., 2003, A revised dislocation model of interseismic deformation of the Cascadia subduction zone: Journal of Geophysical Research, v. 108, p. 1–13, https://doi.org/10.1029/2001JB001227.

Warnock, A.C., Burmester, R.F., and Engebretson, D.C., 1993, Paleomagnetism and tectonics of the Crescent Formation, northern Olympic Mountains, Washington: Journal of Geophysical Research, v. 98, p. 11729–11741, https://doi.org/10.1029/93JB00709.

Washington Geological Survey, 2017, Surface geology, 1:24,000—GIS data, September 2017: Washington Geological Survey Digital Data Series DS-10, version 3.0, previously released November 2016.

Wessel, P., Smith, W.H.F., Scharroo, R., Luis, J., and Wobbe, F., 2013, Generic Mapping Tools: Improved Version Released: Eos (Washington, D.C.), v. 94, p. 409–410, https://doi.org/10.1002/2013EO450001.

Yu, G., Wesnousky, S.G., and Ekström, G., 1993, Slip partitioning along major convergent plate boundaries: Pure and Applied Geophysics, v. 140, p. 183–210, https://doi.org/10.1007/BF00879405.

FIGURE CAPTIONS

Figure 1. Convergent margins of the eastern Pacific Ocean (trenches outlined in white). Cascadia (CAS), Panama (PA) and Bolivia (BOL) all display a concave-outboard trench geometry and show evidence for oroclinal bending in the upper plate (Silver et al., 1990, Allmendinger et al., 2005). Imagery from ESRI DigitalGlobe. Study area outlined with dashed white box.

Figure 2. A: Tectonic setting of the concave-outboard Cascadia subduction zone, showing Juan de Fuca-North America motion (thick arrows, MORVEL; DeMets et al., 2010), and GNSS velocity vectors (thin arrows; error ellipses (0.43 mm/yr mean standard error) omitted for clarity) relative to stable North America (NA) (UNAVCO Plate Boundary Observatory database; McCaffrey et al., 2013). Megathrust interseismic locking pattern from Wang et al. (2003), where the locked zone is dark gray and locking decreases downdip through the effective transition zone

Publisher: GSA
Journal: GEOL: Geology
DOI:10.1130/G45473.1

(lighter gray); B: Generalized geologic setting surrounding the Olympic Mountains (OM), showing geologically-defined axial trace of the orocline (ATO), paleomagnetic declinations (Beck and Engebretson, 1982; Prothero et al., 2008), average orientations of foliations within 23 structural domains (See Data Repository for details), and Quaternary-active crustal faults with modern fault kinematics shown by red arrow pairs (USGS Quaternary Fault and Fold database, http://earthquake.usgs.gov/hazards/qfaults, unless otherwise noted): 1 – Leech River Fault (Morell et al., 2017; Li et al., 2018), 2 – Darrington-Devil's Mountain Fault Zone, 3 – Utsalady Point Fault, 4 – Southern Whidbey Island Fault Zone, 5 – Lake Creek-Boundary Creek Fault (Nelson et al., 2017), 6 – Seattle Fault, 7 – Tacoma Fault, 8 – Saddle Mountain Fault, 9 – Canyon River Fault.

Figure 3. Vertical axis rotations derived from the GNSS velocities in Fig. 2A. Red and blue wedges indicate the sense and magnitude of rotation; small orange wedges show 1-sigma uncertainty. Black and grey wedges show rotations (and uncertainties) derived from paleomagnetic data, assuming bending initiated at ~18 Ma, the onset time of Olympic Mountain uplift (Brandon et al., 1998).

Figure 4. Along-strike changes in subduction obliquity with respect to Juan de Fuca slab depth contours (McCrory et al. 2012), and horizontal compressive stress (S_{Hmax}) directions (Balfour et al. 2011; Heidbach et al. 2016). Black arrows: Juan de Fuca-North America (JDF-NA) relative motion; grey and red arrows: slab contour-normal and parallel (MORVEL; DeMets et al., 2010). Inset: Simplified S_{HMax} orientations (green arrows) relative to the strike and known kinematics of active faults (fault numbering and references as in Fig. 2).

[1]GSA Data Repository item 2018xxx, Figure DR1, Table DR1, and GNSS analysis methods, is available online at http://www.geosociety.org/datarepository/2018/, or on request from editing@geosociety.org.

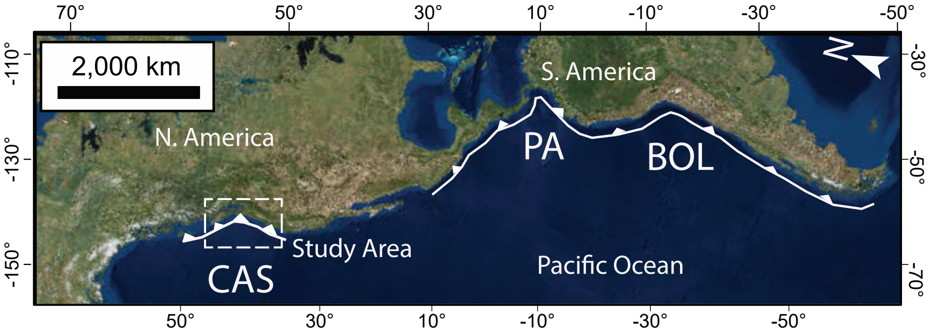

70°
50°
30°
10°
-10°
-30°
-50°
2,000 km
N
S. America
N. America
PA
BOL
Study Area
CAS
Pacific Ocean
-110°
-130°
-150°
-30°
-50°
-70°
50°
30°
10°
-10°
-30°
-50°

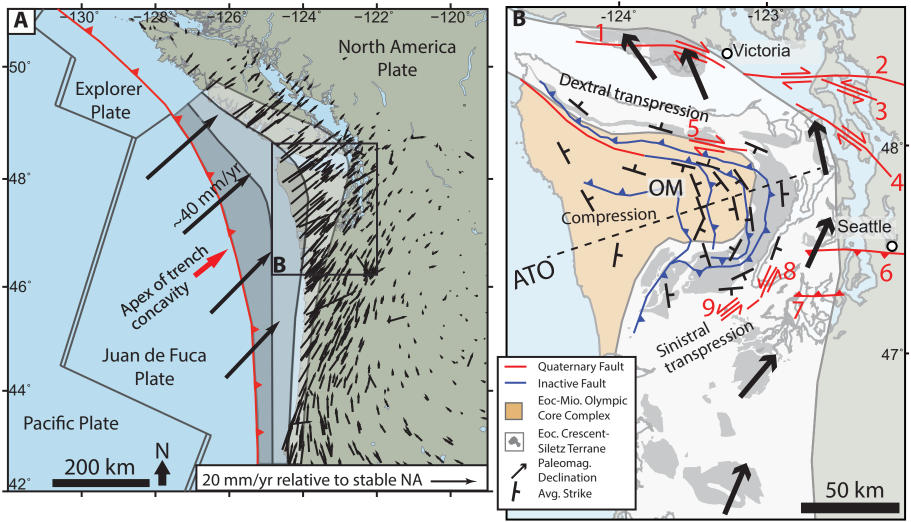

A
−130°
−128°
−126°
−124°
−122°
−120°
50°
48°
46°
44°
42°
North America Plate
Explorer Plate
~40 mm/yr
Apex of trench concavity
Juan de Fuca Plate
Pacific Plate
B
200 km
N
20 mm/yr relative to stable NA
B
−124°
−123°
48°
47°
Victoria
Seattle
Dextral transpression
Compression
Sinistral transpression
OM
ATO
1
2
3
4
5
6
7
8
9
Quaternary Fault
Inactive Fault
Eoc-Mio. Olympic Core Complex
Eoc. Crescent-Siletz Terrane
Paleomag. Declination
Avg. Strike
50 km

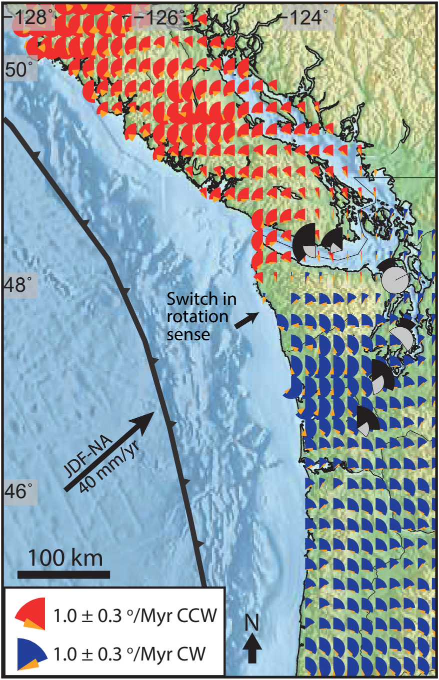

-128°
-126°
-124°
50°
48°
46°
Switch in rotation sense
JDF-NA 40 mm/yr
100 km
N
1.0 ± 0.3 °/Myr CCW
1.0 ± 0.3 °/Myr CW

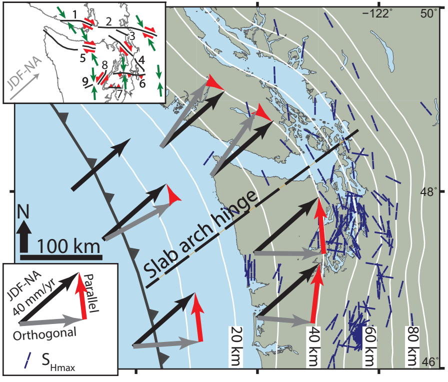

1
2
3
4
5
6
7
8
9
JDF-NA
−122°
50°
48°
46°
N
100 km
Slab arch hinge
JDF-NA
40 mm/yr
Parallel
Orthogonal
S_{Hmax}
20 km
40 km
60 km
80 km